

# Ptbp1 knockdown failed to induce astrocytes to neurons in vivo

Guixiang Yang

Zixiang Yan

Xiaoqing Wu

Meng Zhang

Chunlong Xu

Linyu Shi

Hui Yang

HuiGene Therapeutics Co., Ltd., Shanghai 200131, China; Institute of Neuroscience, Chinese Academy of Sciences; Lingang Laboratory, Shanghai 200031, China; HuiEdit Therapeutics Co., Ltd., Shanghai 2001

<https://orcid.org/0000-0003-3590-722X>

**Kailun Fang** (✉ [fangkailun@sibcb.ac.cn](mailto:fangkailun@sibcb.ac.cn))

Institute of Neuroscience, State Key Laboratory of Neuroscience, Key Laboratory of Primate Neurobiology, CAS Center for Excellence in Brain Science and Intelligence Technology, Shanghai Research Cen

---

## Brief Communication

### Keywords:

**Posted Date:** August 8th, 2022

**DOI:** <https://doi.org/10.21203/rs.3.rs-1817676/v1>

**License:** © ⓘ This work is licensed under a Creative Commons Attribution 4.0 International License.

[Read Full License](#)

---

**Version of Record:** A version of this preprint was published at Gene Therapy on February 1st, 2023. See the published version at <https://doi.org/10.1038/s41434-023-00382-5>.

# Abstract

Conversion of non-neuronal cells to neurons is a promising potential strategy for the treatment of neurodegenerative diseases. Recent studies have reported that shRNA-, CasRx-, or ASO-mediated Ptbp1 suppression could reprogram resident astrocytes to neurons. However, some groups have disputed the data interpretation of the reported neuron conversion events. These controversies surrounding neuron conversion may be due to differences in the astrocyte fate-mapping systems. Here, we suppressed Ptbp1 using Cas13X, and labeled astrocytes with the HA tag fused to Cas13X (Cas13X-NLS-HA). Compared with the GFAP-driven tdTomato labeling system (AAV-GFAP::tdTomato-WPRE) in previous studies, we found no astrocyte-to-neuron conversion in mouse striatum via the HA-tagged labeling system. Our findings indicate Ptbp1 knockdown failed to induce neuron conversion *in vivo*.

# Full Text

Conversion of non-neuronal cells to neurons is a promising potential strategy for the treatment of neurodegenerative diseases. Recent studies have reported that shRNA-, CasRx-, or ASO-mediated Ptbp1 suppression could reprogram resident astrocytes to neurons<sup>1-3</sup>. However, some groups have disputed the data interpretation of the reported neuron conversion events<sup>4-8</sup>. These controversies surrounding neuron conversion may be due to differences in the astrocyte fate-mapping systems. Here, we suppressed Ptbp1 using Cas13X, and labeled astrocytes with the HA tag fused to Cas13X (Cas13X-NLS-HA). Compared with the GFAP-driven tdTomato labeling system (AAV-GFAP::tdTomato-WPRE) in previous studies, we found no astrocyte-to-neuron conversion in mouse striatum via the HA-tagged labeling system. Our findings indicate Ptbp1 knockdown failed to induce neuron conversion *in vivo*.

Previously, we found that CasRx could repress Ptbp1 in astrocytes and induce astrocyte-to-neuron (AtN) conversion<sup>2</sup>. However, technical difficulties in the CasRx-mediated Ptbp1 knockdown reported by other groups<sup>5,8</sup> led us to investigate alternative approaches to repress Ptbp1. To this end, we tested the efficiency of Ptbp1 knockdown by Cas13X, a hyper-compact CRISPR-Cas13 protein with low collateral effect recently identified by our group<sup>9</sup>. We screened five sgRNAs targeting Ptbp1 mRNA (Fig. 1A) and found that sgRNAs-2, -3, and -5, independently or combined, could effectively knock down Ptbp1 expression in HEK293T, Cos7, and N2a cell lines (Fig. 1B).

To estimate whether Ptbp1 could be knocked down by Cas13X *in vivo*, we applied an 1.5E9 vg/injection of AAV-PHP.eB capsid with a 681 bp-length human GFAP promoter<sup>10</sup> to drive astrocyte-specific expression of Cas13X-NLS-HA-sgPtbp1-(2,3,5) or the non-target control (sgNT) in C57BL/6 mice (Fig. 1C, 1D). Immunofluorescent staining of brain sections showed that although the endogenous mouse GFAP signal was unable to maintain for 2 months (Fig. 1E), the Cas13X-HA signal persistently over-expressed (Fig. 1F), and the PTBP1 signal significantly decreased over time (Fig. 1D, 1G), which was indicated by the decreasing proportion of Ptbp1 + HA + GFAP + astrocytes in AAV-GFAP::Cas13X-sgPtbp1 treated mice from 74.79% at 1-week post-injection to 18.42%, 14.96%, 11.98% at 2 weeks, 1 month, and 2 months post-injection, respectively (Fig. 1G). By contrast, the proportion of Ptbp1 + HA + GFAP + astrocytes in AAV-

GFAP::Cas13X-sgNT treated mice was not significantly changed from 1 week to 2 months post-injection (Fig. 1C, 1G). And the Ptbp1 knockdown efficiency of a higher viral dose of 7.5E9 vg/injection is similar to 1.5E9 vg/injection (Figure S1A, S1B).

To determine whether Ptbp1 suppression could successfully induce AtN conversion, the Ptbp1-knockdown virus (AAV-GFAP::Cas13X-sgPtbp1) and astrocyte-tracing virus (AAV-GFAP::tdTomato-WPRE) were co-injected into the striatum of wild-type (WT) mice (Fig. 2A, 2B). At 1 month and 2 months after injection, the populations of tdTomato + NeuN + cells were significantly greater in the Ptbp1 knockdown group compared to that in the non-target control group (10.04% vs 1.02% tdTomato + among total NeuN + cells, respectively; Fig. 2C). These results suggested potential AtN conversion, which was consistent with observations in several previous studies<sup>2,3</sup>. However, the NeuN + cell density was not significantly changed, which indicated that further verification was needed to determine whether AtN conversion occurred (Fig. 2D).

To validate whether the tdTomato labeled neurons were converted from astrocytes, we then applied another labeling system to track astrocytes. The HA tag in the GFAP::Cas13X-NLS-HA-sgPtbp1 construct was used to label astrocytes at 1 month and 2 months post-injection (Fig. 3A, 3B). Different from the results observed from AAV-GFAP::tdTomato-WPRE, immunofluorescent staining revealed that HA + NeuN + cell populations were not significantly different between Ptbp1 knockdown and control mice (Fig. 3A, 3B), indicating no AtN conversion. Since AtN intermediate cells might emerge earlier than 1 month, we also tracked the HA signal at 1 week and 2 weeks post-injection, in the early stages of Ptbp1 suppression. Again, no significant differences in HA + NeuN + cell proportions could be detected between Ptbp1 knockdown and the non-target control group (Fig. 3A, and 3B). Combined together, from 1 week to 2 months, there was no significant change of HA + NeuN + cells among NeuN + cells (0.14% in Ptbp1 KD group vs 0.22% in non-target controls,  $P = 0.2157$ ; Fig. 3C), which aligned well with several recent reports of no AtN conversion in transgenic mouse models<sup>4-6</sup>. In addition, the NeuN + cell density was not significantly changed (Fig. 3D), and no S100 $\beta$  + NeuN + AtN intermediate cell was observed among thousands of S100 $\beta$  + Ptbp1<sup>low</sup> astrocytes from 1 week to 2 months post-injection (Fig. 3E). Taken together, these results indicate that Ptbp1-suppression was not able to convert astrocyte or fibroblast to neuron *in vivo*.

Conversion of non-neuronal cells to neurons by Ptbp1-knockdown has been considered a potential strategy for the treatment of neurodegenerative diseases<sup>1-3</sup>. However, whether astrocytes can be converted to neurons in the brain or in the retina after Ptbp1-knockdown is conflicting<sup>4-8</sup>. Here we applied Cas13X to knockdown Ptbp1, took the HA-tagged labeling system to label astrocytes, and observed no significant changes in the proportion of HA + NeuN + cells, no changes in NeuN + cell density, and no intermediate conversion cells in the Ptbp1 knockout group, indicating that no AtN conversion occurred.

The first question to note is whether Ptbp1 can be knocked down by Cas13. Although CasRx (Cas13d) has been reported to efficiently knockdown genes *in vivo*<sup>2,11-13</sup>, two studies reported quite limited or no Ptbp1 knockdown efficiency mediated by CasRx. One of the possible explanations could be the high

collateral effect of CasRx. Hyperactivity of CasRx with on-targeted sgRNA would lead to cell death, while low expression of CasRx results in low knockdown efficiency<sup>14</sup>. The AAV dose balance of efficacy and toxicity should be carefully controlled. For the technical difficulty of the CasRx application, we discovered a new member of the Cas13 family, Cas13X, to replace CasRx. Here we found 1.5E9 vg/injection of AAV.PHP.eB-GFAP::Cas13X-sgPtbp1 was able to persistently knockdown Ptbp1 from 2 weeks to 2 months post-injection (Fig. 1C, 1D, and 1G). And a 5-fold higher dose of 7.5E9 vg/injection showed the same efficient Ptbp1-suppression (Figure S1B) and no difference from viable neuron number (data not shown), indicating Cas13X was a potential RNA editing tool for in vivo gene therapy.

The second question is whether AtN conversion occurred after the Ptbp1 knockdown. Although two studies showed AtN conversion after Ptbp1 knockdown<sup>2,3</sup>, these results were not reproducible when a different astrocyte-labeling system was applied<sup>4-8</sup>. Here we observed no AtN conversion when Ptbp1 was significantly knocked down by Cas13X when using HA staining to label astrocytes (Fig. 3B-3E). Although significant more TdTomato + NeuN + cells have been found in the Ptbp1-suppressed striatum by AAV-pGFAP::TdTomato-WPRE (Fig. 2B, 2C), this result may be misled by the tracing system.

There are some explanations of how the astrocyte-tracing system affects the AtN results. Although the GFAP promoter was widely applied to label astrocytes in the AtN-success-studies<sup>1-3</sup>, recent studies found the introduction of GFAP promoter resulted in high levels of leaky in neurons, up to 50%<sup>5</sup>. And the AAV-based labeling system increases the leakage of GFAP promoters compared to astrocyte-labeling mouse strains. For instance, the introduction of an endogenous GFAP promoter (in GFAP-Cre; LSL-YFP mouse strain) enabled stringent astrocyte-specific YFP expression, while the exogenous GFAP promoter (in AAV-GFAP-EGFP) was leaky<sup>5</sup>. Since the GFAP promoter is complex and of low specificity, the Aldh1l1 promoter is currently used for astrocyte labeling. There was no AtN conversion under Ptbp1-knockdown when the Aldh1l1 promoter was applied<sup>5,6,8,15</sup>.

In addition, here we also demonstrated that different reporters, such as the GFAP::tdTomato and the HA tag, can generate markedly different outcomes in AtN conversion as well. It would align well with conflicting observations by two previous studies, one used YFP and reported high astrocyte-specificity of a GFAP-CreER<sup>T2</sup>; LSL-YFP mouse strain with no detectable AtN conversion<sup>5</sup>, but in another study, it was observed using tdTomato in a GFAP-CreERTM; Rosa-tdTomato mouse strain<sup>3</sup>. Moreover, the intensity of the reporter on the labeling construct might contribute to GFAP promoter leakage. Removing the WPRE element and decreasing the reporter translation in an AAV-GFAP::tdTomato labeling system was able to increase GFAP promoter specificity in retina<sup>16</sup>. Thus, the type and intensity of reporter in astrocyte labeling systems also warrants careful attention when applied to AtN conversion studies.

The third question is about the significant improvements in animal models of neurodegenerative diseases or retina-degenerative diseases after Ptbp1-knockdown<sup>2,3</sup>. Since there was no AtN conversion, there may have other explanations, including rejuvenation of endogenous neurons in the brain and retina. And the exact mechanism behind the phenotype-rescue should be re-verified in the future.

In summary, the results reported in this study suggest no reprogramming ability of Ptbp1 knockdown *in vivo*. And the mechanism of Ptbp1-knockdown mediated gene therapy should be revisited.

## Materials And Methods

### Vector and gRNA sequences.

The vector sequences were provided in supplementary information. SgPtbp1-2: 5'-tgtggttgagaactggatgtagatgggct-3'; sgPtbp1-3: 5'-gagcccatctggatcagtgccatcttgccg-3'; sgPtbp1-5: 5'-agtcgatgcgagcgtgcagcagcggcgtgt-3'; sgNT: 5'-attggcaccatgccgtgggttcaatattg-3'.

### Cell culture and plasmids transfection

N2a, Cos7, and 293T cell lines were obtained from the Cell Bank of Shanghai Institute of Biochemistry and Cell Biology (SIBCB), Chinese Academy of Sciences (CAS). They were cultured in 37°C and 5% CO<sub>2</sub> incubator in medium DMEM (Gibco) supplemented with 10% fetal bovine serum (FBS, Gibco) and 1 × penicillin/streptomycin (Gibco). 3 µg plasmids were transiently transfected with 6 µl Polyethylenimine (PEI) into cultured cells in 12-well clusters.

### RNA extraction and RT-qPCR

The transfected plasmids containing co-expression elements of mCherry. Three days after transfection, mCherry-positive cells (top 20%) were collected by fluorescence-activated cell sorting (FACS). RNA was extracted with TRIzol Reagent (Ambion). cDNA was obtained with HiScript Q RT SuperMix for qPCR Kit (Vazyme). Quantitative PCR (qPCR) was performed using AceQ qPCR SYBR Green Master Mix (Vazyme) and LightCycler 480 II (Roche).

### Mice

10-week-old male C57BL/6 mice were obtained from Vital River Laboratory Animal Technology Co., Ltd. All animal experiments were performed and approved by the Animal Care and Use Committee of the Institute of Huigene Therapeutics Inc., Shanghai, China.

### AAV package and preparation

Viral particles of AAV-PHP.eB were packaged in co-transfected HEK293T cells with the other two plasmids: pAAV-Rep-Cap and pAAV-Helper. After harvest, viral particles were purified with a heparin column (GE HEALTHCARE BIOSCIENCES) and then concentrated with an Ultra-4 centrifugal filter unit (Amicon, 100,000 molecular weight cutoff). Titers of viral particles were determined by qPCR to achieve >1E12 particles/ml. The AAV titer details were provided in supplementary information.

### Striatum injection

10-week-old male C57BL/6 mice were anesthetized with Zoletil® 50 (Virbac, 0.1ml/10g) and then placed in a stereotaxic mouse frame. The skin over the skull was shaven and opened using a razor. 1.5µl of AAV was injected into the striatum at the following coordinates (relative to bregma): anteroposterior (A/P) = +0.75 mm, mediolateral (M/L) = -1.9 mm, dorsoventral (D/V) = -3.45 mm. The viral solution was injected slowly (300nl/min).

### **Immunofluorescence for brain section**

Immunofluorescence staining was performed at different time points after AAV injection. The brains were perfused and fixed with 4% paraformaldehyde (PFA) overnight and kept in 30% sucrose for at least 12 hours. Brains were sectioned after embedding and freezing, and slices with a thickness of 30 µm were used for immunofluorescence staining. Brain sections were rinsed thoroughly with 0.1 M phosphate buffer (PB). Primary antibodies: Rabbit anti-PTBP1(1:500, PA5-81297, Invitrogen), Rabbit anti-NeuN(1:500, 24307S, Cell Signaling Technology), Mouse anti-NeuN(1:500, AB104224, Abcam), Rat anti-HA(1:500, 11867423001, ROCHE), Mouse anti-GFAP(1:500, AB279290, Abcam), Mouse anti-S100β(1:500, S2532, Merck). Secondary antibodies: Alexa Fluor® 488 AffiniPure Donkey Anti-Rabbit IgG (H+L) (1:1000, 711-545-152, Jackson ImmunoResearch Labs), Alexa Fluor® 488 AffiniPure Donkey Anti-Mouse IgG (H+L)(1:1000, 715-545-151, Jackson ImmunoResearch Labs), Cy<sup>5</sup>™ AffiniPure Donkey Anti-Rat IgG (H+L) (1:1000, 712-175-153, Jackson ImmunoResearch Labs), Cy3 AffiniPure Donkey Anti-Rabbit IgG (H+L) (1:1000, 711-165-152, Jackson ImmunoResearch Labs) were used in this study. After antibody incubation, slides were washed and covered with mountant (Life Technology). Images were visualized under a NIKON C2+ microscope.

## **Declarations**

### **ACKNOWLEDGMENTS**

We thank Weiya Bai and Guannan Geng for AAV vector preparation, and Yanxia Gao and Leping Cheng for project discussion. This work was supported by the Chinese National Science and Technology major project R&D Program of China (2017YFC1001302 and 2018YFC2000101), Strategic Priority Research Program of the Chinese Academy of Science (XDB32060000), National Natural Science Foundation of China (31871502, 31901047, and 82021001), Basic Frontier Scientific Research Program of Chinese Academy of Sciences From 0 to 1 original innovation project (ZDBS-LY-SM001), Lingang Lab (Grant LG202106-01-02), and International Partnership Program of Chinese Academy of Sciences (153D31KYSB20170059).

### **AUTHOR CONTRIBUTIONS**

L.S., H.Y., and K.F. designed the research, G.Y., Z.Y., X.W., and M.Z. performed experiments and analyzed data. C.X., H.Y., and K.F. wrote the manuscript with input from all authors.

### **DECLARATION OF INTERESTS**

Y.H. is a founder of HuiGene Therapeutics Co., Ltd. The remaining authors declare no conflict of interests.

## References

1. Maimon, R., Chillon-Marinas, C., Snethlage, C.E., Singhal, S.M., McAlonis-Downes, M., Ling, K., Rigo, F., Bennett, C.F., Da Cruz, S., Hnasko, T.S., Muotri, A.R., et al. (2021). Therapeutically viable generation of neurons with antisense oligonucleotide suppression of PTB. *Nature neuroscience* *24*, 1089–1099. 10.1038/s41593-021-00864-y.
2. Zhou, H., Su, J., Hu, X., Zhou, C., Li, H., Chen, Z., Xiao, Q., Wang, B., Wu, W., Sun, Y., Zhou, Y., et al. (2020). Glia-to-Neuron Conversion by CRISPR-CasRx Alleviates Symptoms of Neurological Disease in Mice. *Cell*. 10.1016/j.cell.2020.03.024.
3. Qian, H., Kang, X., Hu, J., Zhang, D., Liang, Z., Meng, F., Zhang, X., Xue, Y., Maimon, R., Dowdy, S.F., Devaraj, N.K., et al. (2020). Reversing a model of Parkinson's disease with in situ converted nigral neurons. *Nature* *582*, 550–556. 10.1038/s41586-020-2388-4.
4. Leib, D., Chen, Y.H., Monteys, A.M., and Davidson, B.L. (2022). Limited astrocyte-to-neuron conversion in the mouse brain using NeuroD1 overexpression. *Molecular therapy: the journal of the American Society of Gene Therapy* *30*, 982–986. 10.1016/j.ymthe.2022.01.028.
5. Wang, L.L., Serrano, C., Zhong, X., Ma, S., Zou, Y., and Zhang, C.L. (2021). Revisiting astrocyte to neuron conversion with lineage tracing in vivo. *Cell*. 10.1016/j.cell.2021.09.005.
6. Chen, W., Zheng, Q., Huang, Q., Ma, S., and Li, M. (2022). Repressing PTBP1 fails to convert reactive astrocytes to dopaminergic neurons in a 6-hydroxydopamine mouse model of Parkinson's disease. *eLife* *11*. 10.7554/eLife.75636.
7. Hoang, T., Kim, D.W., Appel, H., Pannullo, N.A., Leavey, P., Ozawa, M., Zheng, S., Yu, M., Peachey, N.S., and Blackshaw, S. (2022). Genetic loss of function of Ptbp1 does not induce glia-to-neuron conversion in retina. *Cell reports* *39*, 110849. 10.1016/j.celrep.2022.110849.
8. Xie, Y., Zhou, J., and Chen, B. (2022). Critical examination of Ptbp1-mediated glia-to-neuron conversion in the mouse retina. *Cell reports* *39*, 110960. 10.1016/j.celrep.2022.110960.
9. Xu, C., Zhou, Y., Xiao, Q., He, B., Geng, G., Wang, Z., Cao, B., Dong, X., Bai, W., Wang, Y., Wang, X., et al. (2021). Programmable RNA editing with compact CRISPR-Cas13 systems from uncultivated microbes. *Nature methods* *18*, 499–506. 10.1038/s41592-021-01124-4.
10. Lee, Y., Messing, A., Su, M., and Brenner, M. (2008). GFAP promoter elements required for region-specific and astrocyte-specific expression. *Glia* *56*, 481–493. 10.1002/glia.20622.
11. He, B., Peng, W., Huang, J., Zhang, H., Zhou, Y., Yang, X., Liu, J., Li, Z., Xu, C., Xue, M., Yang, H., et al. (2020). Modulation of metabolic functions through Cas13d-mediated gene knockdown in liver. *Protein & cell* *11*, 518–524. 10.1007/s13238-020-00700-2.
12. Zhou, C., Hu, X., Tang, C., Liu, W., Wang, S., Zhou, Y., Zhao, Q., Bo, Q., Shi, L., Sun, X., Zhou, H., et al. (2020). CasRx-mediated RNA targeting prevents choroidal neovascularization in a mouse model of age-related macular degeneration. *Natl Sci Rev* *7*, 835–837. 10.1093/nsr/nwaa033.

13. Powell, J.E., Lim, C.K.W., Krishnan, R., McCallister, T.X., Saporito-Magrina, C., Zeballos, M.A., McPheron, G.D., and Gaj, T. (2022). Targeted gene silencing in the nervous system with CRISPR-Cas13. *Science advances* 8, eabk2485. [10.1126/sciadv.abk2485](https://doi.org/10.1126/sciadv.abk2485).
14. Tong, H., Huang, J., Xiao, Q., He, B., Dong, X., Liu, Y., Yang, X., Han, D., Wang, Z., Ying, W., Zhang, R., et al. (2021). High-fidelity Cas13 variants for targeted RNA degradation with minimal collateral effect. [2021.2012.2018.473271](https://doi.org/10.1101/2021.12.18.473271). [10.1101/2021.12.18.473271](https://doi.org/10.1101/2021.12.18.473271) bioRxiv.
15. Hoang, T., Kim, D.W., Appel, H., Pannullo, N.A., Leavey, P., Ozawa, M., Zheng, S., Yu, M., Peachey, N.S., Kim, J., and Blackshaw, S. (2021). Ptp1 deletion does not induce glia-to-neuron conversion in adult mouse retina and brain. [2021.2010.2004.462784](https://doi.org/10.1101/2021.10.04.462784). [10.1101/2021.10.04.462784](https://doi.org/10.1101/2021.10.04.462784) bioRxiv.
16. Gao, Y., Fang, K., Yan, Z., Zhang, H., Geng, G., Wu, W., Xu, D., Zhang, H., Zhong, N., Wang, Q., Cai, M., et al. (2022). Develop an efficient and specific AAV based labeling system for Muller glia in mice. [2021.2012.2010.472182](https://doi.org/10.1101/2021.12.10.472182). [10.1101/2021.12.10.472182](https://doi.org/10.1101/2021.12.10.472182) bioRxiv.

## Figures



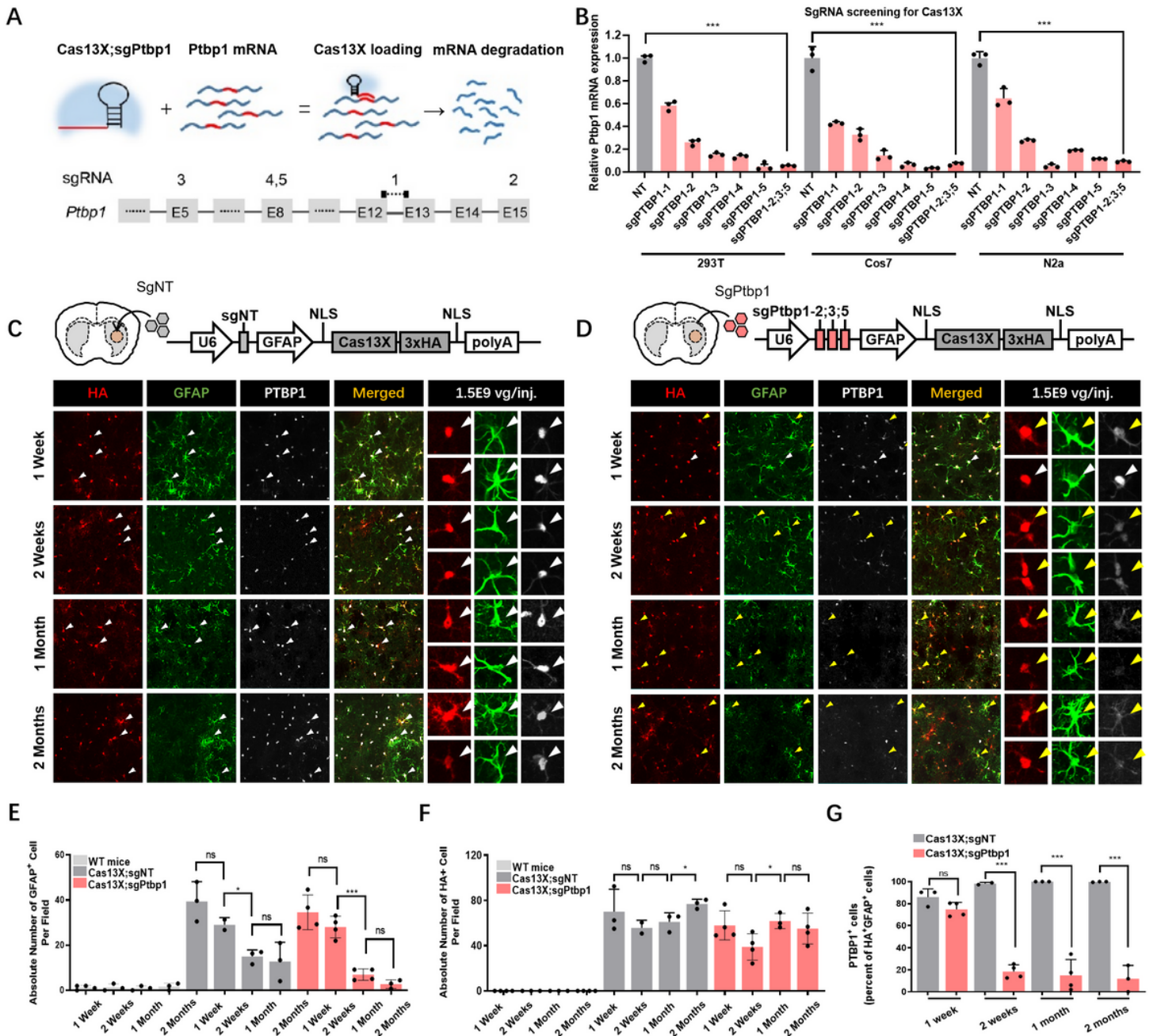
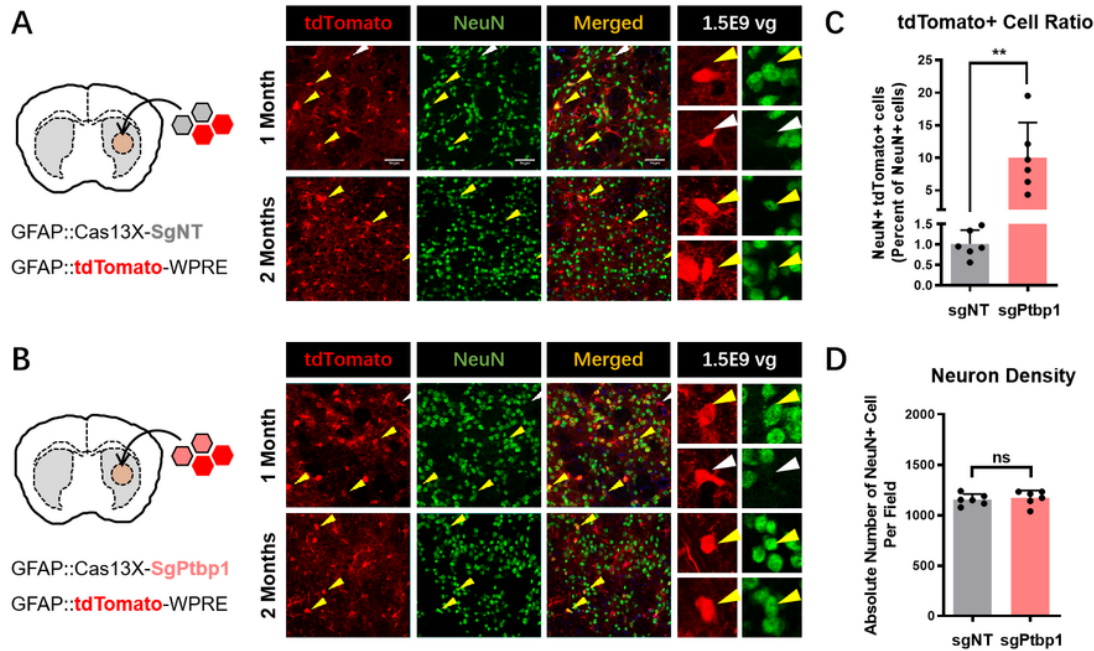


Figure 1

### Ptpb1-knockdown by Cas13X and sgRNA *in vitro* and *in vivo*

(A) Schematic of Cas13X mode of knockdown and Ptpb1 sgRNA design targeting exons 5, 8, 12, 13 and 15. (B) Relative mRNA expression of Ptpb1 under treatments with Cas13X;sgPtpb1 or Cas13X;sgNT in 293T, Cos7, and N2a cell lines. \*\*\*: P value<0.0001 in two-tailed t-test. (C-D) Representative images of striatum sections after AAV-Cas13X-sgNT (C) or AAV-Cas13X-sgPtpb1 (D) injection (1.5E9 vg/injection) with immunofluorescent staining for HA, GFAP, and Ptpb1. White arrowheads: cells without Ptpb1 suppression. Yellow arrowheads: Ptpb1-suppressed cells. NT: non-target control. (E) An absolute number

of endogenous GFAP+ cells at 1, 2, 4, and 8 weeks post-injection. **(F)** Absolute numbers of exogenous HA+ cells at 1, 2, 4, and 8 weeks post-injection. **(G)** Quantification and statistical analysis of Ptbp1+ cell proportions among HA+GFAP+ cells, indicating Ptbp1 knockdown efficiency in AAV-transduced astrocytes. Significance was determined by a two-tailed t-test. \*  $P < 0.05$ , \*\*\*  $P < 0.001$ , ns: not significant.



**Figure 2**

**Astrocyte-to-Neuron conversion after Ptbp1 knockdown validated by tdTomato mediated astrocyte-labeling system.**

**(A-B)** Representative images of striatum sections after AAV-Cas13X-sgNT **(A)** or AAV-Cas13X-sgPtbp1 administration **(B)** coinjected with AAV-GFAP::tdTomato-WPRE. Striatum sections were stained for NeuN. Yellow arrowheads: NeuN+ tdTomato+ cells. White arrowheads: NeuN- tdTomato+ cells. NT: non-target control. **(C)** Quantification and statistical analysis of tdTomato+ NeuN+ proportions among NeuN+ cells from 2 weeks to 2 months post-injection. **(D)** Absolute numbers of NeuN+ cells from 2 weeks to 2 months after injection with AAV-Cas13X-sgNT or AAV-Cas13X-sgPtbp1 and tdTomato AAV. Significance was determined by a two-tailed t-test. \*\*  $P < 0.01$ , ns: not significant. NT: non-target control.

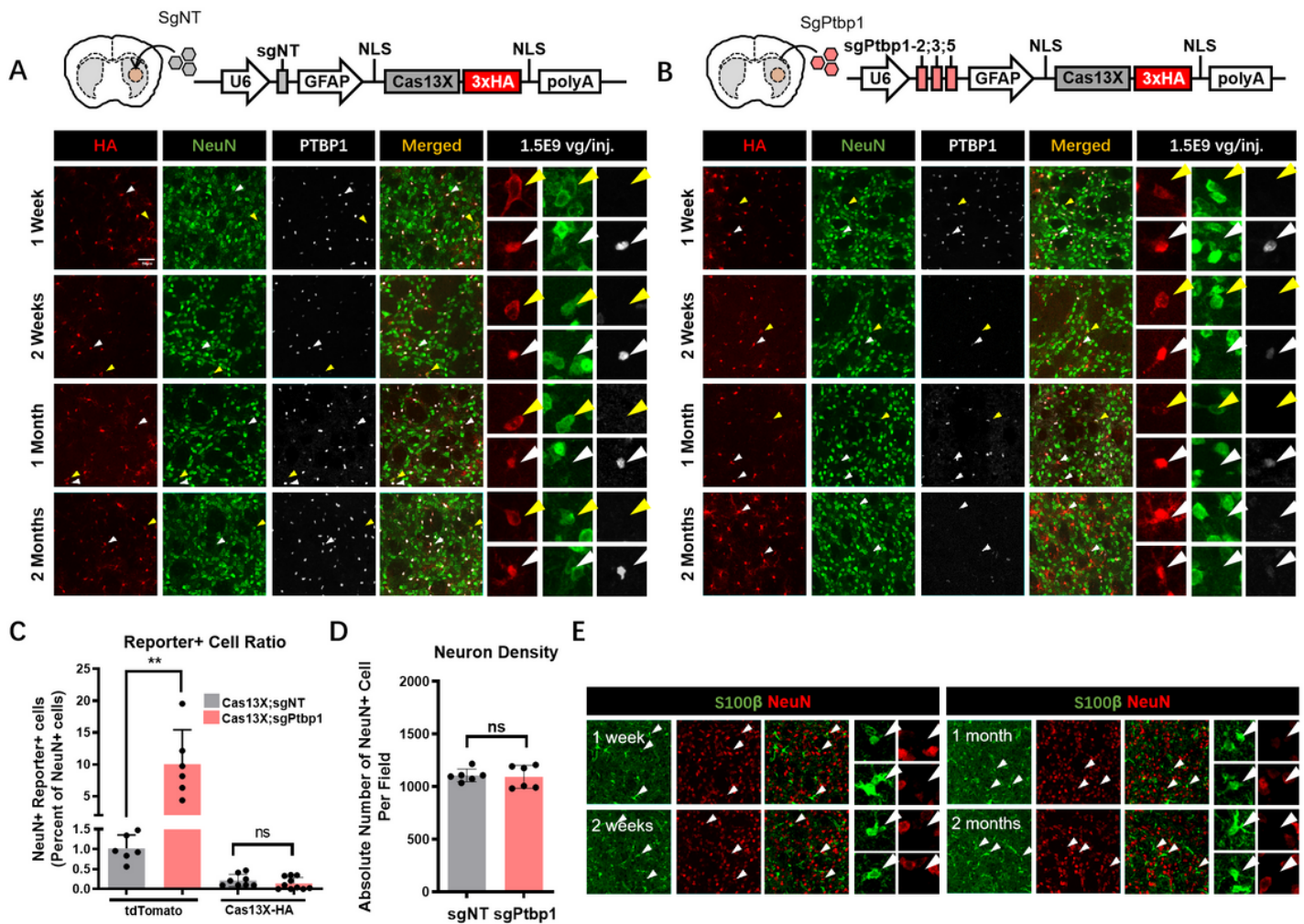


**Figure 3**

**No astrocyte-to-Neuron conversion occurred after Ptpb1 knockdown validated by HA mediated astrocyte labeling system.**

**(A-B)** Representative images of striatum sections after AAV-Cas13X-sgNT **(A)** or AAV-Cas13X-sgPtpb1 administration **(B)**. Striatum sections were stained for NeuN, HA, and Ptpb1. Yellow arrowheads: HA+ NeuN+ cells. White arrowheads: HA+ NeuN- cells. NT: non-target control. **(C)** Quantification and statistical analysis of reporter+ NeuN+ proportions among NeuN+ cells from 2 weeks to 2 months post-injection. The reporter was tdTomato in AAV-GFAP::tdTomato-WPRE, or HA in AAV-GFAP::Cas13X-NLS-HA **(D)** Absolute numbers of NeuN+ cells from 2 weeks to 2 months after injection with AAV-Cas13X-sgNT or AAV-Cas13X-sgPtpb1. **(E)** Representative images of brain sections at different time points after AAV-Cas13X-sgNT or AAV-Cas13X-sgPtpb1 treatment. White arrowheads: S100β+ NeuN- cells. WT mice, wild-type littermate mice without AAV treatment. Significance was determined by a two-tailed t-test. \* P<0.05, \*\* P<0.01, \*\*\* P<0.001, ns: not significant.

## Supplementary Files

This is a list of supplementary files associated with this preprint. Click to download.

- [20220701SupplementarynoAtNconversion.docx](#)